Experimental Demonstration of Quantum Teleportation of Broadband Squeezing

Hidehiro Yonezawa,[1,2] Samuel L. Braunstein,[3] and Akira Furusawa[1,2]

[1]*Department of Applied Physics, School of Engineering, The University of Tokyo, 7-3-1 Hongo, Bunkyo-ku, Tokyo 113-8656, Japan*
[2]*CREST, Japan Science and Technology (JST) Agency, 1-9-9 Yaesu, Chuo-ku, Tokyo 103-0028, Japan*
[3]*Computer Science, University of York, York YO10 5DD, United Kingdom*

(Received 31 May 2007; published 14 September 2007)

We demonstrate an unconditional high-fidelity teleporter capable of preserving the broadband entanglement in an optical squeezed state. In particular, we teleport a squeezed state of light and observe -0.8 ± 0.2 dB of squeezing in the teleported (output) state. We show that the squeezing criterion translates directly into a sufficient criterion for entanglement of the upper and lower sidebands of the optical field. Thus, this result demonstrates the first unconditional teleportation of broadband entanglement. Our teleporter achieves sufficiently high fidelity to allow the teleportation to be cascaded, enabling, in principle, the construction of deterministic non-Gaussian operations.

DOI: 10.1103/PhysRevLett.99.110503 PACS numbers: 03.67.Hk, 03.65.Ud, 03.67.Mn, 42.50.Dv

One of the most significant developments in quantum optics in recent years, which promises to revolutionize the field, has been the move from online evolution to the use of offline resources with detection and feedforward [1] to achieve the same (and often superior) result. Here, online refers to the direct unitary evolution of a signal, as contrasted with the use of an auxiliary quantum system (an offline resource) that is coupled to the original signal and whose measurement yields some classical information about that signal. This information is processed offline and used to modify the signal (in a feedforward step).

This approach was demonstrated, for example, in the making of a near-ideal phase-insensitive amplifier [2], an achievement that would be virtually impossible with the direct (online) use of a laser amplifier. Similarly, squeezing of anything other than vacuum states has been virtually impossible until the recent realization that the squeezed resources could be moved offline and replaced with a feedforward scheme [3,4]. This opens the door for near-ideal quantum nondemolition measurements that have long been championed for gravity-wave detection and quantum metrology more generally [4]. In fact, one of the earliest examples of a feedforward protocol is quantum teleportation [5]. Here there is an entangled (offline) resource, Bell-state detection, and feedforward. In ideal teleportation the teleported state reproduces the input state, thus implementing the identity evolution or gate. It was later realized that by modifying the entangled resource, other quantum gates could be implemented [6]. While this applies equally to both discrete and continuous-variable (CV) systems, the latter's ability to construct non-Gaussian gates would supplement linear optics and deliver universal quantum computation in the CV setting. In particular, a cascaded teleportation protocol would allow for the construction of a (nonlinear) cubic phase gate [7,8].

Since the first demonstration of teleportation in the late 1990s [9], we have seen remarkable progress in teleportation related technologies. In particular, in the CV setting, experiments teleporting coherent states of light [10–14] and matter [15], as well as halves of entangled states (entanglement swapping) [13] and squeezed states [16] have all been reported. In the entanglement swapping experiment the entanglement was shared between two spatially separated modes. By contrast, in the experiment reported here the entanglement lies between upper and lower sidebands of the same spatial mode [17,18]. Hence the entire entangled state is teleported. In the experiment teleporting squeezed states [16], the states were teleported with a fidelity exceeding the classical limit [19]. Nonetheless, squeezing itself was not preserved in the output state [16]. By contrast, the teleportation reported here maintains the squeezing and the entanglement in the output state. This is a prerequisite for any cascaded teleportation protocol, and indeed for any multistep information processing scheme.

For the CV teleportation experiments described above (including entanglement swapping), no more than -3 dB of squeezing has been required. However, in order to maintain squeezing at the output, at least -4.8 dB of squeezing is essential. While high levels of squeezing have been generated in the past (recently up to -9 dB [20]), we report here the first application of such high levels of squeezing. This represents a significant breakthrough in phase stabilization.

It is not surprising that the teleportation of an entire entangled state, as reported here, necessarily entails the preservation of squeezing in the (output) teleported state. In fact, when the squeezing criterion is decomposed into quadrature amplitudes of the upper and lower sidebands, it translates directly into a sufficient criterion for entanglement between these sidebands [21,22]

$$\Delta_{\mathrm{sq}} \equiv \langle (\Delta[\hat{x}(\Omega_s) + \hat{x}(-\Omega_s)])^2 \rangle + \langle (\Delta[\hat{p}(\Omega_s) - \hat{p}(-\Omega_s)])^2 \rangle < 1. \quad (1)$$

Here $\Delta\hat{O}$ denotes the uncertainty in $\hat{O}$, Ω_s is the side band frequency, and $\hat{x}(\pm\Omega_s)$ and $\hat{p}(\pm\Omega_s)$ are canonically conjugate quadrature operators for the two sideband modes, obeying the uncertainty relation

$\langle[\Delta\hat{x}(\pm\Omega_s)]^2\rangle\langle[\Delta\hat{p}(\pm\Omega_s)]^2\rangle \geq \frac{1}{16}$ (with $\hbar = \frac{1}{2}$) [17,22]. In our experiment, we estimate a value of $\Delta_{\rm sq} = 0.83 \pm 0.04$ for the teleported states ($\Delta_{\rm sq} = 0.24 \pm 0.01$ for the input state), demonstrating successful unconditional quantum teleportation of entanglement. This is the first such *unconditional* demonstration for either discrete or continuous quantum variables.

The CV quantum optical field may be described in terms of the annihilation operator for the electromagnetic field $\hat{a}(t)$ or its Fourier transform $\hat{a}(\Omega)$, here written in the rotating frame about the central optical frequency. From these the sideband quadrature operators may be defined in terms of the annihilation and creation operators for the sideband modes as $\hat{x}(\Omega) = \frac{1}{2}[\hat{a}(\Omega) + \hat{a}^\dagger(\Omega)]$ and $\hat{p}(\Omega) = \frac{i}{2}[\hat{a}^\dagger(\Omega) - \hat{a}(\Omega)]$. These sideband quadratures satisfy the usual canonical commutation relations $[\hat{x}(\Omega), \hat{p}(\Omega')] = \frac{i}{2}\delta(\Omega - \Omega')$. In the experiment, we treat the four sideband operators $\hat{x}(\pm\Omega_s)$ and $\hat{p}(\pm\Omega_s)$ at the sideband frequency Ω_s or combinations of these operators. Homodyne detectors measure $\hat{x}_{\rm hom}(t) \equiv \hat{a}(t) + \hat{a}^\dagger(t)$ which in the frequency (or rf) domain has the form [17]

$$\hat{x}_{\rm hom}(\Omega) \equiv \hat{a}(\Omega) + \hat{a}^\dagger(-\Omega) = \hat{x}(\Omega) + \hat{x}(-\Omega) + i[\hat{p}(\Omega) - \hat{p}(-\Omega)]. \quad (2)$$

The rf in-phase (real) and rf out-of-phase (imaginary) parts of $\hat{x}_{\rm hom}(\Omega)$ may be extracted simultaneously and are used for the feedforward step of the teleportation. In addition, a spectrum analyzer is used to measure the noise power (the sum of the variances of both real and imaginary components) of this homodyne signal [23]

$$\langle(\Delta[\hat{x}(\Omega) + \hat{x}(-\Omega)])^2\rangle + \langle(\Delta[\hat{p}(\Omega) - \hat{p}(-\Omega)])^2\rangle. \quad (3)$$

At the sideband frequency $\Omega = \Omega_s$ this noise power is just $\Delta_{\rm sq}$ from our entanglement criterion (1). Thus, when the noise level in the spectrum analyzer shows broadband squeezing below the vacuum level, it also indicates the presence of entanglement between upper and lower sidebands. In other words, if the teleported state preserves squeezing below the vacuum level, then the teleported state also preserves entanglement between the sidebands.

Figure 1 shows the experimental setup for CV quantum teleportation of an electromagnetic field mode. We use three optical parametric oscillators (OPOs) which contain periodically poled $KTiOPO_4$ as a nonlinear medium. The output of a Ti:sapphire laser at 860 nm is frequency doubled in an external cavity containing a 10 mm long potassium niobate crystal. The output beam at 430 nm is divided into three beams to pump three OPOs. The pump powers are around 120 mW for OPO3 and around 100 mW for OPO1 and OPO2. OPO1 and OPO2 are used to generate the EPR beams. The third OPO is used to generate the quadrature-squeezed input state (except when teleporting a coherent state, in which case the input is generated by modulating a weak coherent beam from the laser at frequency sidebands of 1 MHz).

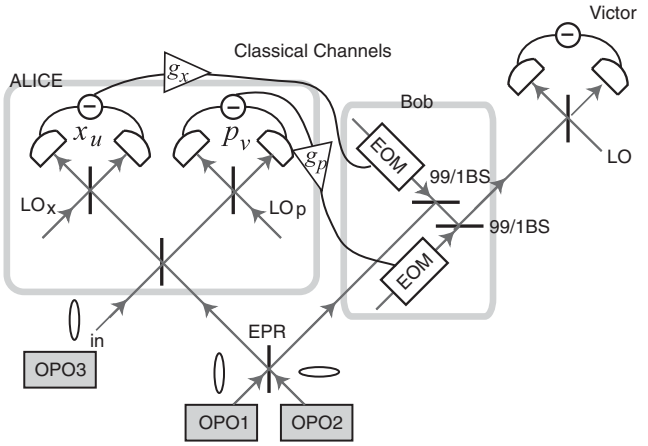

FIG. 1. Experimental setup for CV quantum teleportation. OPOs are optical parametric oscillators. EOMs are electro-optical modulators. All beam splitters except those labeled as 99/1 BSs are 50/50. LOs are local oscillators for homodyne detection.

Here we summarize the broadband description of teleportation as may be found in Ref. [24], but other than the mixing of upper and lower sidebands in the original shared EPR entangled states and in the homodyne detection, it is very close to the single mode description [10–13,16,25]. In particular, CV teleportation requires one of the EPR beams to be sent to Alice ($\hat{x}_A(\Omega)$, $\hat{p}_A(\Omega)$), and the other to Bob ($\hat{x}_B(\Omega)$, $\hat{p}_B(\Omega)$). Alice makes a joint homodyne measurement between her EPR beam ($\hat{x}_A(\Omega)$, $\hat{p}_A(\Omega)$) and the input beam ($\hat{x}_{\rm in}(\Omega)$, $\hat{p}_{\rm in}(\Omega)$), and sends her homodyne measurement results ($x_u(\Omega)$, $p_v(\Omega)$) to Bob through classical channels. Bob receives Alice's measurement results and "displaces" his EPR beam ($\hat{x}_B(\Omega)$, $\hat{p}_B(\Omega)$) to reconstruct the input state.

The gains of the classical channels are defined as $g_x = \langle\hat{x}_{\rm out}\rangle/\langle\hat{x}_{\rm in}\rangle$ and $g_p = \langle\hat{p}_{\rm out}\rangle/\langle\hat{p}_{\rm in}\rangle$, respectively, (over the same rf bandwidths), where ($\hat{x}_{\rm out}$, $\hat{p}_{\rm out}$) describes the output mode. We set the gains to near unity, obtaining $g_x = 1.00 \pm 0.01$ and $g_p = 1.00 \pm 0.01$ (see Ref. [12] for the tuning procedure). These gains remained fixed throughout the experiment. The visibilities of the homodyne detectors were about 98%.

For unity gain and no losses, the output mode may be written as [13,24]

$$\hat{x}_{\rm out}(\Omega_s) = \hat{x}_{\rm in}(\Omega_s) - [\hat{x}_A(\Omega_s) - \hat{x}_B(-\Omega_s)]$$
$$\hat{p}_{\rm out}(\Omega_s) = \hat{p}_{\rm in}(\Omega_s) + [\hat{p}_A(\Omega_s) + \hat{p}_B(-\Omega_s)]. \quad (4)$$

In the ideal case, EPR beams satisfy $\hat{x}_A(\Omega_s) - \hat{x}_B(-\Omega_s) \to 0$ and $\hat{p}_A(\Omega_s) + \hat{p}_B(-\Omega_s) \to 0$, yielding a teleported state that is identical to the input state. Treating all three squeezed states as pure with the same squeezing parameter r, the variances of the teleported state become

$$\langle(\Delta\hat{x}_{\rm out})^2\rangle = \frac{3}{4}e^{-2r}, \qquad \langle(\Delta\hat{p}_{\rm out})^2\rangle = \frac{e^{2r} + 2e^{-2r}}{4}, \quad (5)$$

compared with the variances of a vacuum mode [22]

$\langle(\Delta\hat{x}_{\rm vac})^2\rangle = \langle(\Delta\hat{p}_{\rm vac})^2\rangle = \frac{1}{4}$. Therefore in order to observe squeezing at the output, $e^{-2r} < \frac{1}{3}$ should be satisfied, corresponding to at least -4.8 dB squeezing.

As a means of calibrating the performance of our teleporter, we use the mean fidelity $F_{\rm coh} = \langle\alpha|\rho_{\rm out}|\alpha\rangle$ for teleporting coherent states (of coherent amplitude α) yielding output states $\rho_{\rm out}$. For a coherent state and unity gain, the fidelity can then be estimated from the variances of the outputs [13]

$$F_{\rm coh} = \frac{2}{\sqrt{[1 + 4\langle(\Delta\hat{x}_{\rm out})^2\rangle][1 + 4\langle(\Delta\hat{p}_{\rm out})^2\rangle]}}. \quad (6)$$

Figure 2 shows the results of teleportation of a coherent state. Plots (a) and (b) show the noise power of the input and output states (for the x quadrature; p quadrature not shown), measured by a spectrum analyzer. We use EPR beams created from a pair of squeezed vacua of around -6 dB each. Ideally, that level of squeezing would yield a fidelity $F_{\rm coh} = 0.8$, and would enable cascading the teleportation scheme 4 times [26]. If cascaded, such a high-fidelity teleporter with a photon number detector would then allow for the construction of a deterministic non-Gaussian gate like a cubic phase gate [7,8] for CVs.

In fact, achieving such a high-fidelity teleporter poses significant technical challenges. Indeed, although high levels of squeezing are in themselves feasible (recently up to -9 dB [20]), such high levels of squeezing in a real experiment (such as teleportation) would require very good phase locking. As mentioned above, to realize our high-fidelity teleporter, we were able to generate and use -6 dB squeezing. For experiments using high squeezing levels, the antisqueezed quadrature easily contaminates

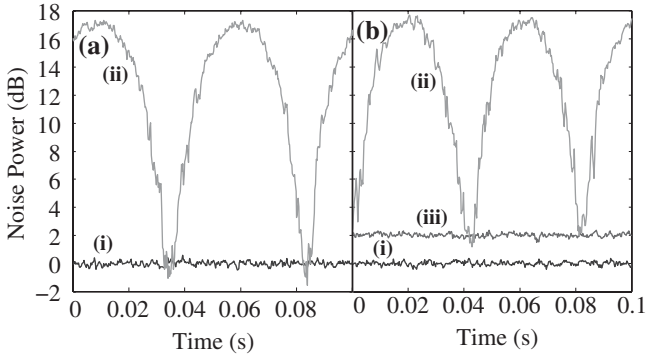

FIG. 2. Quantum teleportation of a coherent state. Plots (a) and (b) show the measurement results by a spectrum analyzer. Plot (a) shows the input coherent state. Trace (i) shows vacuum noise level. Trace (ii) shows the input coherent state with the phase scanned. Plot (b) shows the output state of the teleportation for the x quadrature (p quadrature not shown). Trace (i) plots the vacuum noise level. Trace (ii) plots the results of the teleportation with the phase of the input coherent state scanned. Trace (iii) plots the variance for teleported vacuum. All traces except traces (ii) are averaged 30 times. The center frequency is 1 MHz. The resolution and video bandwidths are 30 kHz and 300 Hz, respectively.

the squeezed quadrature [20]. Hence, unusually high mechanical stability of the experimental setup was needed to avoid such degradation in the squeezing.

To measure the input state, we block Alice's EPR beam and lock Alice's two homodyne detectors to the same quadrature simultaneously. The difference current from her two detectors was fed into a spectrum analyzer. In these measurements, the phase of the input coherent state was scanned. The maximum noise amplitude of the input state was found to be around 17 dB (corresponding to a coherent amplitude of $\alpha \simeq 3.5$). In Fig. 2(b) the maximum noise amplitude of the output of the teleported state was also around 17 dB, confirming the near unit gains of the classical channels. The variances of the output quadratures were measured separately as [22], $\langle(\Delta\hat{x}_{\rm out})^2\rangle = 2.0 \pm 0.2$ dB and $\langle(\Delta\hat{p}_{\rm out})^2\rangle = 2.3 \pm 0.2$ dB relative to the vacuum. These results are in good agreement with theoretical values 2.1 and 2.2 dB which are calculated from experimental losses and separately measured EPR correlations $\langle[\Delta(\hat{x}_A - \hat{x}_B)]^2\rangle = -5.6 \pm 0.2$ dB and $\langle[\Delta(\hat{p}_A + \hat{p}_B)]^2\rangle = -5.5 \pm 0.2$ dB. Using the above variances and Eq. (6), we obtain near-ideal fidelity $F_{\rm coh} = 0.76 \pm 0.02$ for our teleporter, exceeding the classical limit $F_{\rm coh} = \frac{1}{2}$ [19,27,28], the no-cloning limit $F_{\rm coh} = \frac{2}{3}$ [29], and the highest fidelity reported to date [13].

We now describe the teleportation of a squeezed state. Figure 3(a) shows the input squeezed state measured by a spectrum analyzer. The variances of the input state's squeezed and antisqueezed quadratures are -6.2 ± 0.2 dB and 12.0 ± 0.2 dB, respectively. The EPR correlations are as good as those obtained in the teleportation of a coherent state. The squeezed output state is shown in Fig. 3(b). The measured variances of the output state are -0.8 ± 0.2 dB and 12.4 ± 0.2 dB for the x and p quadratures, respectively. These values are in good agreement with theoretical calculations, indicating a high degree of mechanical stability in our phase-locking system. (For comparison, the teleportation was repeated with squeezing in the p quadrature, yielding -0.3 ± 0.2 dB squeezing in the output.) These levels of subvacuum noise measured in the output clearly demonstrate that the squeezing (and hence the entanglement) is preserved in the process of teleportation.

Figures 3(c) and 3(d) show the reconstructed Wigner functions of the input and output states. Here the Wigner function is defined as [30]

$$W(x, p) = \frac{1}{\pi}\int d\Delta e^{-2ip\Delta}\langle x + \Delta/2|\hat{\rho}|x - \Delta/2\rangle. \quad (7)$$

To reconstruct the Wigner function, we follow the procedures described in Ref. [31]. We record 1 MHz sideband components with a 30 kHz bandwidth by an analog-to-digital converter (sampling rate 300 kHz, around 100 000 points collected with the local oscillator phase scanned). We then calculate the Wigner function by the inverse Radon transformation [30,31].

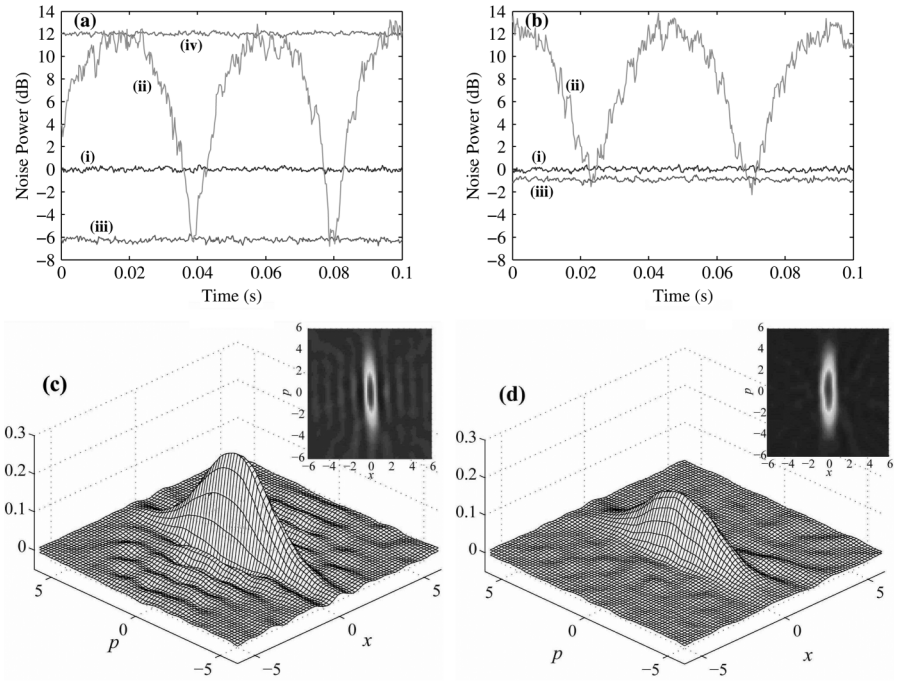

FIG. 3. Quantum teleportation of a squeezed state. Plots (a) and (b) show the measurements from a spectrum analyzer. Plot (a) shows the squeezed state to be teleported. Trace (i) plots the vacuum noise level. Trace (ii) plots the squeezed state with phase scanned. Traces (iii) and (iv) show the squeezed state with phase locked to the squeezed and antisqueezed quadratures. Plot (b) shows the output state of the teleportation for the x quadrature (p quadrature not shown). Trace (i) plots the vacuum noise level. Trace (ii) plots the teleported state with the input state's phase scanned. Trace (iii) plots the teleported state with the input state's phase locked to the x quadrature. All traces except traces (ii) are averaged 30 times. Plots (c) and (d) show the Wigner functions of the input and output states of the teleportation, respectively.

In summary, we have demonstrated quantum teleportation of a squeezed state of light that preserves the squeezing from input to output and estimate the squeezing obtained at the output as $\Delta_{\mathrm{sq}} = 0.83 \pm 0.04$. We also show that the teleported state preserves the entanglement between the upper and lower sidebands. The successful preservation of entanglement through a teleportation channel hinges upon the existence of a high-fidelity teleporter, which requires high levels of squeezing in each of three modes. This technically challenging achievement opens a new door for CV quantum information processing. In particular, high-fidelity teleporters will enable the transport, preservation, and manipulation of highly non-Gaussian states [7,8] such as single-photon states or superpositions of pairs of coherent states [32–34].

This work was partly supported by the MEXT of Japan. S. L. B. acknowledges support from the Wolfson Royal Society Research Merit scheme.

[1] J. Mertz *et al.*, Phys. Rev. Lett. **64**, 2897 (1990).
[2] V. Josse *et al.*, Phys. Rev. Lett. **96**, 163602 (2006).
[3] J. Yoshikawa *et al.*, arXiv:quant-ph/0702049.
[4] R. Filip, P. Marek, and U. L. Andersen, Phys. Rev. A **71**, 042308 (2005).
[5] C. H. Bennett *et al.*, Phys. Rev. Lett. **70**, 1895 (1993).
[6] D. Gottesman and I. L. Chuang, Nature (London) **402**, 390 (1999).
[7] A. Furusawa and N. Takei, Phys. Rep. **443**, 97 (2007).
[8] D. Gottesman, A. Kitaev, and J. Preskill, Phys. Rev. A **64**, 012310 (2001).
[9] Science editors, Science **282**, 2157 (1998).
[10] A. Furusawa *et al.*, Science **282**, 706 (1998).
[11] W. P. Bowen *et al.*, Phys. Rev. A **67**, 032302 (2003).
[12] T. C. Zhang *et al.*, Phys. Rev. A **67**, 033802 (2003).
[13] N. Takei *et al.*, Phys. Rev. Lett. **94**, 220502 (2005).
[14] H. Yonezawa, T. Aoki, and A. Furusawa, Nature (London) **431**, 430 (2004).
[15] J. F. Sherson *et al.*, Nature (London) **443**, 557 (2006).
[16] N. Takei *et al.*, Phys. Rev. A **72**, 042304 (2005).
[17] J. Zhang, Phys. Rev. A **67**, 054302 (2003).
[18] E. H. Huntington and T. C. Ralph, J. Opt. B **4**, 123 (2002).
[19] S. L. Braunstein *et al.*, J. Mod. Opt. **47**, 267 (2000).
[20] Y. Takeno *et al.*, Opt. Express **15**, 4321 (2007).
[21] L. M. Duan *et al.*, Phys. Rev. Lett. **84**, 2722 (2000).
[22] All broadband quantities involve an implicit integration over a small bandwidth—the detector resolution—and are normalized with respect to one-half of the vacuum noise level—except when quoted in dB, where they are relative to the vacuum.
[23] R. A. Witte, *Spectrum and Network Measurements* (Prentice-Hall, New Jersey, 1993).
[24] P. van Loock, S. L. Braunstein, and H. J. Kimble, Phys. Rev. A **62**, 022309 (2000).
[25] S. L. Braunstein and H. J. Kimble, Phys. Rev. Lett. **80**, 869 (1998).
[26] S. Suzuki *et al.*, Appl. Phys. Lett. **89**, 061116 (2006).
[27] S. L. Braunstein *et al.*, Phys. Rev. A **64**, 022321 (2001).
[28] K. Hammerer *et al.*, Phys. Rev. Lett. **94**, 150503 (2005).
[29] F. Grosshans and P. Grangier, Phys. Rev. A **64**, 010301(R) (2001).
[30] U. Leonhardt, *Measuring the Quantum State of Light* (Cambridge University Press, Cambridge, U.K., 1997).
[31] G. Breitenbach and S. Schiller, J. Mod. Opt. **44**, 2207 (1997).
[32] A. Ourjoumtsev *et al.*, Science **312**, 83 (2006).
[33] J. S. Neergaard-Nielsen *et al.*, Phys. Rev. Lett. **97**, 083604 (2006).
[34] K. Wakui *et al.*, Opt. Express **15**, 3568 (2007).